Check for updates

View Article Online
View Journal

Chemical Science

Accepted Manuscript

This article can be cited before page numbers have been issued, to do this please use: L. Zhou, Y. Zhang, Y. Li, T. Yang, Z. Chu, Q. Zhang, H. Tang, A. Ma, P. Gao, C. Wang, Y. Wong, C. Liu, S. Shen, J. Zhang, Q. Shi, H. Tang and J. Wang, *Chem. Sci.*, 2026, DOI: 10.1039/D6SC00255B.

This is an Accepted Manuscript, which has been through the Royal Society of Chemistry peer review process and has been accepted for publication.

Accepted Manuscripts are published online shortly after acceptance, before technical editing, formatting and proof reading. Using this free service, authors can make their results available to the community, in citable form, before we publish the edited article. We will replace this Accepted Manuscript with the edited and formatted Advance Article as soon as it is available.

You can find more information about Accepted Manuscripts in the Information for Authors.

Please note that technical editing may introduce minor changes to the text and/or graphics, which may alter content. The journal's standard Terms & Conditions and the Ethical guidelines still apply. In no event shall the Royal Society of Chemistry be held responsible for any errors or omissions in this Accepted Manuscript or any consequences arising from the use of any information it contains.

ROYAL SOCIETY OF CHEMISTRY

rsc.li/chemical-science

View Article Online
DOI: 10.1039/D6SC00255B

Chemoproteomics Unveils the Antibacterial Mechanism of Silver Ions: Inhibiting Peptidoglycan Synthesis via Targeting Mur Family Proteins in *Staphylococcus aureus*

Lirun Zhou[a,b,#], Ying Zhang[b,c,#], Yajian Li[d], Tong Yang[b], Zheng Chu[b], Qianyu Zhang[b], Hechen Tang[b], Ang Ma[b], Peng Gao[b], Chen Wang[b], Yin Kwan Wong[e], Cui Liu[b], Shengnan Shen[b], Junzhe Zhang[b], Qiaoli Shi[b], Huan Tang[b,*], and Jigang Wang[a,b,c,*]

[a] Guangdong Basic Research center of Excellence for Integrated Traditional and Western Medicine for Qingzhi Diseases, Guangdong provincial Key Laboratory of Chinese Medicine pharmaceutics, School of Traditional Chinese Medicine and School of pharmaceutical Sciences, Southern Medical University, Guangzhou, Guangdong, 510515, China.

[b] State Key Laboratory for Quality Ensurance and Sustainable Use of Dao-di Herbs, Artemisinin Research Center, and Institute of Chinese Materia Medica, China Academy of Chinese Medical Sciences, Beijing 100700, China.

[c] Department of Pulmonary and Critical Care Medicine, Shenzhen Institute of Respiratory Diseases, and Shenzhen Clinical Research Centre for Geriatrics, Shenzhen People's Hospital, First Affiliated Hospital of Southern University of Science and Technology, Second Clinical Medical College of Jinan University, Shenzhen, Guangdong, 518020, China.

[d] Department of Urology, National Cancer Center/National Clinical Research Center for Cancer/Cancer Hospital, Chinese Academy of Medical Sciences and Peking Union Medical College, 100021, Beijing, China.

[e] Department of Pharmacology, Yong Loo Lin School of Medicine, National University of Singapore, Singapore 117543, Singapore.

[#] These authors contributed equally to this work.

[*] Corresponding authors. E-mail addresses: htang@icmm.ac.cn (H. Tang), jgwang@icmm.ac.cn (J. Wang).

Open Access Article. Published on 23 April 2026. Downloaded on 6/26/2026 5:23:11 PM.
This article is licensed under a Creative Commons Attribution-NonCommercial 3.0 Unported Licence.

Chemical Science Accepted Manuscript

View Article Online
DOI: 10.1039/D6SC00255B

Open Access Article. Published on 23 April 2026. Downloaded on 6/26/2026 5:23:11 PM.
This article is licensed under a Creative Commons Attribution-NonCommercial 3.0 Unported Licence.

Abstract

Silver ions (Ag^{+}) have long been employed as natural antimicrobial agents, yet their precise mechanism of action remains unclear. In this study, we show that Ag^{++} displays strong antibacterial activity against *Staphylococcus aureus* (*S. aureus*), including methicillin-resistant strains (MRSA). Using chemoproteomic analysis, we identified MurB, MurC, and MurD as direct coordinate covalent targets of Ag^{+} in *S. aureus*, with binding occurring at cysteine residues Cys224, Cys368, and Cys221, respectively. This interaction leads to a reduction in MurB and MurD expression and inhibits MurC enzymatic activity, ultimately disrupting peptidoglycan synthesis and compromising bacterial cell wall integrity. Consequently, Ag^{+} treatment results in bacterial membrane leakage, altered membrane potential, and inhibited biofilm formation. Additionally, Ag^{+} reduces bacterial adhesion and invasion, alleviating the inflammatory response in host cells. Notably, Ag^{+} exhibits a low resistance frequency compared to conventional antibiotics, underscoring its potential as an effective antimicrobial agent. Its distinct mechanism of action and reduced likelihood of resistance development indicate that it may serve not only as an effective therapeutic strategy, but also as a probe for elucidating the mechanism of bacterial peptidoglycan biosynthesis. These results offer new insights for the development of antibiotics targeting Mur family proteins.

Keywords: Silver, *Staphylococcus aureus*, Multi-omics, Mur family proteins, Peptidoglycan synthesis, Antimicrobial resistance.

Chemical Science Accepted Manuscript

View Article Online
DOI: 10.1039/D6SC00255B

Open Access Article. Published on 23 April 2026. Downloaded on 6/26/2026 5:23:11 PM.
This article is licensed under a Creative Commons Attribution-NonCommercial 3.0 Unported Licence.

Chemical Science Accepted Manuscript

Introduction

Staphylococcus aureus (*S. aureus*), a Gram-positive bacterium, is a leading cause of infectious diseases in both hospital and community settings worldwide. It is closely linked to significant morbidity and mortality, as well as considerable economic burden (1-3). *S. aureus* infected can lead to severe clinical manifestations, including endocarditis, localized wound infections, sepsis, and pneumonia, conditions that may, in some cases, prove fatal (4-6). This challenge is further exacerbated by the rapid rise of antibiotic-resistant strains, particularly MRSA, against which conventional therapies are increasingly ineffective (7). By 2019, MRSA was associated with more than 100,000 deaths across over 200 countries, leading the World Health Organization (WHO) to designate it as a critical priority pathogen in urgent need of new antibiotic development (8-9). This escalating challenge, coupled with the stagnation in antibiotic innovation and extended timelines for new drug development, underscores the critical need for therapeutic agents with distinct mechanisms of action against *S. aureus*.

Silver has a long-standing history in medicinal applications. Historical records, including the Compendium of Materia Medica, document its purported therapeutic properties, such as calming internal organs, soothing the mind, relieving convulsions, and expelling pathogenic factors. In modern scientific research, silver ions (Ag^+) have been confirmed to demonstrate strong antibacterial effects and have yielded encouraging therapeutic results in the management of gastritis, malaria, and parasitic infections (10). Ag^+ is known to interact with bacterial proteins, preferentially binding to cysteine residues, which can lead to degradation of nucleic acids and proteins, disruption of metabolic processes, and ultimately, bacterial cell death (11,12). Clinically, Ag^+-based formulations are already utilized for preventing and treating bacterial infections, including those associated with burns and scalds (13). Moreover, multiple studies have reported that Ag^+ compromises bacterial membranes and cell walls, contributing to its broad-spectrum antimicrobial properties (12). However, despite its well-documented efficacy, the specific protein targets through which Ag^+ exerts its bactericidal effects remain largely unidentified.

View Article Online
DOI: 10.1039/D6SC00255B

Open Access Article. Published on 23 April 2026. Downloaded on 6/26/2026 5:23:11 PM.
This article is licensed under a Creative Commons Attribution-NonCommercial 3.0 Unported Licence.

S. aureus cell wall is predominantly composed of peptidoglycan (approximately 90%) and teichoic acid (about 10%), which collectively maintain bacterial structural integrity, homeostasis, and resistance to external stressors (14). This structure is indispensable for bacterial colonization, infection, and overall survival (15). Peptidoglycan biosynthesis in *S. aureus* proceeds through a multi-step pathway, with the cytoplasmic stages primarily catalyzed by the Mur enzyme family (MurA-MurF). These enzymes sequentially facilitate the formation of UDP-N-acetylmuramyl-pentapeptide (UDP-MurNAc-pentapeptide), an essential precursor for peptidoglycan assembly (**Figure S1**) (16). Notably, genetic studies have confirmed that *S. aureus* can't survive in the absence of functional Mur proteins, underscoring their essential role in bacterial viability (17). Accordingly, the development of small-molecule inhibitors targeting Mur enzymes offers a promising approach for new antibiotic discovery. Although several compounds have demonstrated inhibitory activity against Mur enzymes *in vitro* (18-19), no drugs directed at this family have reached clinical use. Therefore, advancing antibiotics that target Mur proteins may significantly expand our therapeutic arsenal against antibiotic-resistant bacterial infections.

In this study, we systematically evaluated the antibacterial activity and selectivity of Ag^+ against both susceptible and resistant *S. aureus*, including MRSA. Using quantitative chemoproteomics, we globally mapped the protein targets of Ag^+ in *S. aureus* and, for the first time, identified MurB, MurC, and MurD as its direct covalent targets. We further characterized the specific binding of Ag^+ to cysteine residues, Cys224 in MurB, Cys368 in MurC, and Cys221 in MurD, which leads to the suppression of MurB and MurD expression and inhibition of MurC enzymatic activity, thereby disrupting peptidoglycan synthesis. Electron microscopy confirmed that Ag^+ induces marked thinning and rupture of the bacterial wall. Notably, Ag^+ exhibited a low propensity for resistance development in *S. aureus* and demonstrated strong bactericidal effects against amoxicillin-resistant strains. Collectively, this work elucidates key antibacterial targets of Ag^+ and offers a mechanistic foundation for the development of new antibiotics targeting Mur family proteins to combat the global challenge of bacterial resistance.

Chemical Science Accepted Manuscript

View Article Online
DOI: 10.1039/D6SC00255B

Open Access Article. Published on 23 April 2026. Downloaded on 6/26/2026 5:23:11 PM.
This article is licensed under a Creative Commons Attribution-NonCommercial 3.0 Unported Licence.

Chemical Science Accepted Manuscript

Results

Ag^+ Exhibits Potent and Selective Antibacterial Activity

To assess the antibacterial efficacy of Ag^+, we first examined its inhibitory effects against *S. aureus* and MRSA in comparison with amoxicillin. After 24 h of treatment, Ag^+ exhibited potent activity with IC_{50} values of 0.96 μM for *S. aureus* and 6.8 μM for MRSA (**Figure 1A-B**). In contrast, while amoxicillin was highly effective against the drug-sensitive strain (IC_{50} = 19.3 nM), its activity was substantially diminished against MRSA (IC_{50} = 56.8 μM) (**Figure S2**, **Figure 1C**). A checkerboard assay revealed a marked synergistic interaction between Ag^+ and amoxicillin, yielding a fractional inhibitory concentration (FIC) index of 0.127, well below the 0.5 threshold for synergy (**Figure 1D**). Against the Gram-negative bacterium *Escherichia coli* (*E. coli*), Ag^+ displayed an IC_{50} of 13.84 μM (**Figure S3**), indicating a broader, though more potent anti-Gram-positive, spectrum of activity. Further characterization using plate colony counting confirmed a concentration-dependent reduction in *S. aureus* survival (**Figure 1E**). Growth curve analysis demonstrated that Ag^+ suppressed bacterial proliferation in a dose-dependent manner, with growth almost completely inhibited at 2 μM (**Figure 1F**). The *S.areus* killing curve established that Ag^+ at 2 and 4 μM eradicated most bacteria within 12 hours (**Figure 1G**). To assess the biocompatibility of Ag^+, we evaluated its cytotoxicity in human lung epithelial (BEAS-2B) and macrophage (RAW 264.7) cell lines. The 50% cytotoxic concentration (CC_{50}) values were 116.4 μM and 99.74 μM, respectively (**Figure 1H-I**), both substantially higher than the minimum inhibitory concentration (MIC) of Ag^+ against *S. aureus* (2 μM). This broad selectivity window highlights the potential of Ag^+ as a bactericidal agent with favorable cytocompatibility.

Chemoproteomic Profiling Identifies MurB, MurC, and MurD as Direct Targets of Ag^+ in *S. aureus*

To clarify the molecular mechanism of the antibacterial activity of Ag^+, we applied a chemoproteomic approach to identify its direct protein targets in *S. aureus*. Given

View Article Online
DOI: 10.1039/D6SC00255B

Open Access Article. Published on 23 April 2026. Downloaded on 6/26/2026 5:23:11 PM.
This article is licensed under a Creative Commons Attribution-NonCommercial 3.0 Unported Licence.

prior evidence suggesting Ag^+ interacts with cysteine residues (20), we utilized iodoacetamide-alkyne (IAA-yne), an activity-based cysteine probe, in conjunction with activity-based protein profiling (ABPP). This approach enables the identification of covalent protein targets through potential *in situ* bioactivation or direct binding events (21,22). Following the workflow outlined in **Figure 2A**, we systematically profiled Ag^+-binding proteins by assessing changes in cysteine reactivity in the presence or absence of Ag^+. Proteins captured by IAA-yne were fluorescently tagged via copper(I)-catalyzed azide-alkyne cycloaddition (CuAAC). Pre-incubation with Ag^+ resulted in a dose-dependent reduction in fluorescence labeling intensity (**Figure 2B-C**), indicating that Ag^+ covalently occupies cysteine residues in multiple proteins.

To identify these targets, desthiobiotin iodoacetamide (DBIA)-captured proteins were enriched, digested, and subjected to dimethyl labeling for quantitative proteomic analysis. Peptides bearing cysteines were precisely quantified, revealing potential Ag^+-binding proteins based on reduced DBIA labeling upon Ag^+ competition (**Figure 2D**). Notably, three Mur family enzymes, MurB, MurC, and MurD, were identified as prominent candidate targets, as Ag^+ almost completely abolished DBIA binding to these proteins (**Figure 2E**). Gene Ontology (GO) analysis revealed that proteins targeted by Ag^+ were significantly enriched in pathways associated with metal ion binding, catalytic activity, metabolic processes, and cell wall macromolecule biosynthesis (**Figure 2F**), further supporting the functional relevance of the identified targets. To validate these interactions, we overexpressed and purified recombinant MurB, MurC, and MurD. Fluorescence labeling assays with IAA-yne confirmed that Ag^+ effectively competed for binding to all three proteins (**Figure 3A-C**). Moreover, Ag^+ treatment significantly enhanced the thermal stability of MurB (**Figure 3D-E**), MurC (**Figure 3F-G**), and MurD (**Figure 3H-I**), as demonstrated by protein-based thermal shift assays. Furthermore, protein-based thermal shift assays demonstrated that sodium acetate at the same ionic strength does not enhance the thermal stability of MurB, MurC, or MurD (**Figure S5A-C**). These findings collectively establish MurB, MurC, and MurD as direct and biologically relevant targets of Ag^+ in *S. aureus*.

Chemical Science Accepted Manuscript

View Article Online
DOI: 10.1039/D6SC00255B

Open Access Article. Published on 23 April 2026. Downloaded on 6/26/2026 5:23:11 PM.
This article is licensed under a Creative Commons Attribution-NonCommercial 3.0 Unported Licence.

Chemical Science Accepted Manuscript

Ag^+ Specifically Binds to Cys224 of MurB, Cys368 of MurC, and Cys221 of MurD

Our chemoproteomic analysis revealed that Ag^+ covalently interacts with specific cysteine residues: Cys224 in MurB, Cys368 in MurC, and Cys221 in MurD (**Figure 2D**). To elucidate the binding mode, we performed molecular docking simulations, which demonstrated that Ag^+ forms ionic bonds with key residues in each protein: Cys224 and Val227 in MurB (**Figure 4A**), Ile396 and Cys368 in MurC (**Figure 4B**), and Cys221 and Glu230 in MurD (**Figure 4C**), consistent with our mass spectrometry results. To experimentally validate these binding sites, we generated and purified point mutants of each protein: MurB (C224A), MurC (C368A), and MurD (C221A). *In vitro* fluorescence labeling assays showed that Ag^+ lost its ability to compete with IAA-yne labeling in all three mutants (**Figure 4D-F**), confirming the essential role of these cysteine residues in Ag^+ binding. We further quantified the binding affinity using microscale thermophoresis (MST). Ag^+ bound to wild-type MurB with a K_d of 1.8 μM, which decreased 6.6-fold to 12 μM for the MurB(C224A) mutant (**Figure 4G**). Similarly, the binding affinities for wild-type MurC and MurD were 0.65 μM and 0.85 μM, respectively, but decreased more than 10-fold for the MurC(C368A) (8.2 μM, **Figure 4H**) and MurD(C221A) (9.2 μM, **Figure 4I**) mutants. To exclude the influence of ionic strength on the binding affinity between Ag^+ and MurB, MurC, and MurD, we performed MST using sodium acetate at the same concentration. The results showed that, at equivalent ionic strength, no measurable binding was detected between sodium acetate and MurB, MurC, or MurD (**Figure S6A-C**). These findings further indicate that Ag^+ exhibits strong binding interactions with MurB, MurC, and MurD. To provide direct evidence of binding, we employed MALDI-TOF mass spectrometry. Upon addition of Ag^+, the mass-to-charge ratio of MurC increased from 50242.75 to 50456.86 (**Figure 4J**), corresponding to a mass increase of 214.11 Da, approximately equivalent to two Ag^+ atoms. This suggests that one MurC protein molecule can directly bind two Ag^+ ions. Taken together, these findings provide strong evidence that Ag^+ directly and covalently interacts with MurB, MurC, and MurD, with Cys224, Cys368, and Cys221 serving as the primary binding sites, respectively.

View Article Online
DOI: 10.1039/D6SC00255B

Open Access Article. Published on 23 April 2026. Downloaded on 6/26/2026 5:23:11 PM.
This article is licensed under a Creative Commons Attribution-NonCommercial 3.0 Unported Licence.

Chemical Science Accepted Manuscript

Ag^+ Suppresses Expression and Function of Mur Family Proteins

Having established the direct binding of Ag^+ to MurB, MurC, and MurD, we next investigated the functional consequences of these interactions in *S. aureus*. To evaluate the effects of Ag^+ on the biological functions of *S. aureus* without compromising bacterial viability, we treated the cells with sub-IC_{50} concentrations of Ag^+ for 12 h. Subsequently, using a comprehensive proteomic approach, we assessed global protein expression changes following Ag^+ treatment. Volcano plot analysis revealed significant alterations, with 126 proteins upregulated and 128 downregulated (**Figure 5A**). GO analysis indicated that upregulated proteins were primarily associated with ion transport and peptidoglycan-based cell wall processes (**Figure 5B**), while downregulated proteins were enriched in pathways including metal ion stress response, protein folding, and peptidoglycan catabolism (**Figure 5C**). We specifically examined the protein levels of key Mur family enzymes in Ag^+-treated *S. aureus*. In proteomic analysis demonstrated that Ag^+ significantly suppressed the expression of MurA2, MurB, MurE, and MurD (**Figure 5D**). Interestingly, despite direct binding to MurC, its protein expression was upregulated following Ag^+ treatment (**Figure 5D**). This Ag^+-mediated upregulation of MurC may represent a compensatory mechanism in bacteria. We speculate that Ag^+ may interact with the cysteine residue of MurC, thereby inhibiting its enzymatic activity and impairing its function, which in turn triggers this compensatory response. To examine this hypothesis, we evaluated MurC enzymatic activity in the presence of Ag^+. Our results showed that Ag^+ significantly inhibited MurC activity with an IC_{50} of 5.6 μM (**Figure 5E**, **Figure S4**). Furthermore, compared to WT MurC, the enzymatic activity of the MurC (C368A) mutant was markedly reduced (**Figure 5F**), indicating that Cys368 is critical for MurC catalytic function. Importantly, Ag^+ failed to inhibit the enzymatic activity of the MurC (C368A) mutant (**Figure 5G**), confirming that Cys368 serves as the key site through which Ag^+ suppresses MurC activity. Collectively, these findings demonstrate that Ag^+ exerts its antibacterial effects by binding to MurB, MurC, and MurD, thereby inhibiting both the expression of MurB and MurD and the enzymatic activity of MurC. Through this multi-faceted mechanism, Ag^+ disrupts peptidoglycan synthesis and compromises *S. aureus*

View Article Online
DOI: 10.1039/D6SC00255B

cell wall integrity, ultimately resulting in bacterial cell death.

Ag^+ Disrupts Cell Wall Integrity and Induces Bacterial Membrane Damage in *S. aureus*

As essential enzymes in peptidoglycan biosynthesis, MurB, MurC, and MurD collectively play a role in maintaining the structural integrity of the bacterial cell wall (23). To determine whether Ag^+ binding to these targets affects their physiological function, we first quantified *S. aureus* peptidoglycan content. Our results confirmed that Ag^+ significantly inhibits peptidoglycan synthesis (**Figure 6A**). Given that peptidoglycan constitutes 50–85% of the *S. aureus* cell wall, its reduced synthesis is expected to severely compromise cell wall stability (24,25). We next employed transmission and scanning electron microscopy to visualize morphological changes. Untreated bacteria displayed intact, smooth surfaces, whereas Ag^+-treated *S. aureus* showed deformed and collapsed morphologies, indicative of severe cell wall damage (**Figure 6B**). To further visually observe the effects of Ag^+ on the bacterial wall, Ag^+-treated *S. aureus* cells were processed for TEM imaging of ultrathin sections. The results further confirmed severe structural damage, including substantial thinning and rupture of the cell wall (**Figure 6C**).

To evaluate membrane integrity, we performed live/dead staining was conducted using Calcein-AM and propidium iodide. With increasing Ag^+ concentrations, green fluorescence (viable cells) progressively decreased while red fluorescence (nonviable cells) intensified (26,27), confirming Ag^+-induced loss of membrane integrity (**Figure 6D**). Alkaline phosphatase (AKP), an enzyme located between the membrane and cell wall, is released upon cell wall disruption (28-30). After Ag^+ treatment, extracellular AKP levels significantly increased (**Figure 6E**), while intracellular AKP decreased correspondingly (**Figure 6F**), indicating compromised *S. aureus* cell wall barrier function. Membrane potential was assessed using rhodamine dye, which accumulates extracellularly when membrane integrity is impaired (31). Ag^+ treatment markedly enhanced fluorescence intensity (**Figure 6G**), confirming disruption of membrane potential. Finally, we detected substantial leakage of proteins and nucleic acids from

Open Access Article. Published on 23 April 2026. Downloaded on 6/26/2026 5:23:11 PM.
This article is licensed under a Creative Commons Attribution-NonCommercial 3.0 Unported Licence.

Chemical Science Accepted Manuscript

View Article Online
DOI: 10.1039/D6SC00255B

Ag^+-treated *S. aureus* (**Figure 6H-I**), providing direct evidence of membrane permeabilization. Collectively, these results demonstrate that Ag^+, through coordinate covalent interactions with Mur family proteins, disrupts peptidoglycan synthesis and compromises bacteria wall integrity. This results in disruption of membrane potential, increased permeability, and leakage of intracellular components, ultimately resulting in *S. aureus* death.

Ag^+ Attenuates the Virulence of *S. aureus*

The virulence of *S. aureus* is primarily due to its capacity to form biofilms, adhere to and invade host cells, and elicit inflammatory responses (32-34). Since bacterial wall integrity is crucial for these virulence-associated behaviors (35,36), we hypothesized that Ag^+-induced *S. aureus* wall damage would attenuate bacterial pathogenicity. To test this, we first assessed the impact of Ag^+ on *S. aureus* adhesion and invasion of BEAS-2B cells. Ag^+ pretreatment significantly reduced both adhesion (**Figure 7A-B**) and invasion (**Figure 7C-D**) in a concentration-dependent manner, as shown by decreased *S. aureus* colony counts. Consistent with reduced virulence, Ag^+ treatment also alleviated *S. aureus*-induced cytotoxicity in BEAS-2B cells (**Figure 7E**). We further examined the effect on the inflammatory response induced by *S. aureus* infection. Infection significantly elevated secretion of key inflammatory mediators, nitric oxide (NO), interleukin-1β (IL-1β), tumor necrosis factor (TNF-α), and interleukin-6 (IL-6), in BEAS-2B cells. Ag^+ pretreatment effectively suppressed this pro-inflammatory response in a concentration-dependent manner (**Figure 7F-I**). Given the importance of biofilms in persistent infections and antibiotic resistance (35), we assessed biofilm formation using crystal violet staining. Ag^+ potently inhibited biofilm development, achieving over 80% inhibition at a concentration of 0.12 μM (**Figure 7J**). Moreover, Ag^+ exhibited no bactericidal activity against *S. aureus* at any of the biofilm tested concentrations (**Figure S7**), further confirming Ag^+ inhibited biofilm formation is not attributable to bacterial killing. In summary, these findings demonstrate that Ag^+, by disrupting bacterial wall synthesis through targeting Mur family proteins, significantly impairs multiple virulence traits of *S. aureus*, including adhesion, invasion,

Open Access Article. Published on 23 April 2026. Downloaded on 6/26/2026 5:23:11 PM.
This article is licensed under a Creative Commons Attribution-NonCommercial 3.0 Unported Licence.

Chemical Science Accepted Manuscript

View Article Online
DOI: 10.1039/D6SC00255B

biofilm formation, and induction of inflammatory responses. This multifaceted attenuation of pathogenicity, combined with direct bactericidal activity, highlights the potential of Ag^+ as a promising anti-virulence agent.

Ag^+ Demonstrates a Low Propensity for Resistance Development in *S. aureus*

The emergence of multidrug-resistant "superbugs" is frequently driven by the widespread overuse of conventional antibiotics (37). Many frontline therapies against Gram-positive pathogens, including vancomycin, carry inherent risks of resistance development and potential adverse effects (38). We therefore sought to evaluate the potential for *S. aureus* to develop resistance to Ag^+. Using a serial passage assay, we continuously exposed *S. aureus* to sub-inhibitory concentrations (IC_{50}) of Ag^+ or amoxicillin over multiple generations. Resistance to amoxicillin emerged as early as the eighth passage, with the IC_{50} increasing more than 15-fold after 15 generations (**Figure 8A**). In stark contrast, *S. aureus* exhibited no significant development of resistance to Ag^+ throughout the entire experimental period (**Figure 8B**). Notably, Ag^+ maintained potent antibacterial activity against amoxicillin-resistant *S. aureus* even after 14 passages (**Figure 8C**). These findings indicate that Ag^+, through its unique mechanism of targeting Mur family proteins, possesses a distinct advantage in mitigating the development of antibiotic resistance, highlighting its potential as a sustainable antimicrobial agent.

Discussion

The escalating prevalence of antibiotic-resistant pathogens, especially MRSA, presents a significant challenge to global public health. As conventional antibiotics increasingly lose efficacy against evolving resistance mechanisms, the creation of antimicrobial agents with new mechanisms of action becomes imperative (39-40). Within this framework, our study systematically investigates the antibacterial potential of Ag^+, a historically recognized antimicrobial agent with documented therapeutic efficacy in traditional medicine. We demonstrate that Ag^+ exhibits robust and selective antibacterial efficacy against both susceptible and resistant *S. aureus* strains, while

Open Access Article. Published on 23 April 2026. Downloaded on 6/26/2026 5:23:11 PM.
This article is licensed under a Creative Commons Attribution-NonCommercial 3.0 Unported Licence.

Chemical Science Accepted Manuscript

View Article Online DOI: 10.1039/D6SC00255B

showing a markedly low propensity for resistance development. Notably, Ag^+ operates through a distinctive mechanism by covalently targeting Mur family proteins, representing a significant departure from conventional antibiotic strategies, providing a novel perspective for the rational development of new antibiotics targeting Mur family proteins.

The antibacterial potency of Ag^+ is particularly remarkable when evaluated against clinical pathogens. The IC_{50} values of 0.96 μM for *S. aureus* and 6.81 μM for MRSA indicate superior inhibitory activity compared to several reported natural antibacterial compounds, including gallinamide A, cinnamaldehyde, and triptolide (41-43). This enhanced efficacy is especially evident when contrasted with amoxicillin, which, despite its potent activity against drug-sensitive *S. aureus* (IC_{50} = 19.28 nM), shows significantly reduced efficacy against MRSA (IC_{50} = 56.79 μM). The ability of Ag^+ to maintain potent bactericidal activity against amoxicillin-resistant strains, coupled with its significantly lower susceptibility to resistance development, underscores its potential as an effective therapeutic alternative. Furthermore, the broad-spectrum nature of Ag^+, demonstrating activity against both Gram-positive (*S. aureus*) and Gram-negative (*E. coli*) bacteria, highlights its multifunctional antimicrobial character, a particularly valuable attribute in an era of escalating multidrug resistance.

The mechanism of action of Ag^+ represents a significant departure from conventional antibiotics. Our chemoproteomic analysis identified MurB, MurC, and MurD as primary coordinate covalent targets of Ag^+ in *S. aureus*. Specifically, we demonstrate that Ag^+ binds to cysteine residues Cys224, Cys368, and Cys221 in MurB, MurC, and MurD, respectively, thereby disrupting bacterial peptidoglycan synthesis, an innovative approach to bacterial suppression. This targeting strategy gains further support from the observation that Ag^+ exerts significantly stronger bactericidal effects on *S. aureus* (containing 90% peptidoglycan) than on *E. coli* (with only 5-20% peptidoglycan) (44), confirming the particular importance of peptidoglycan synthesis inhibition in its anti-staphylococcal activity.

Notably, the bacterial cell wall constitutes a structure unique to prokaryotic organisms, absent in human cells. This fundamental difference explains the favorable

Open Access Article. Published on 23 April 2026. Downloaded on 6/26/2026 5:23:11 PM.
This article is licensed under a Creative Commons Attribution-NonCommercial 3.0 Unported Licence.

Chemical Science Accepted Manuscript

View Article Online
DOI: 10.1039/D6SC00255B

selectivity of Ag^+, which exhibits potent antibacterial activity while maintaining low cytotoxicity toward mammalian cells, a crucial advantage for therapeutic development. Our GO pathway analysis further reveals that the interaction between Ag^+ and Mur family proteins are involved not only in cell wall biosynthesis but also in other critical processes, including glycolysis and amino acid metabolism. The unique coordinate covalent binding mode between Ag^+ and Mur enzymes offers a novel strategic approach for developing antibiotics that function through mechanisms distinct from currently employed therapeutics. In summary, our results establish that Ag^+ inhibits peptidoglycan synthesis and compromises the bacterial cell wall in S. aureus through a multi-faceted mechanism: reducing MurB and MurD protein levels while directly inhibiting MurC enzymatic activity. This coordinated attack on cell wall integrity leads to impaired biofilm formation, diminished bacterial adherence and invasion capacity, and ultimately, loss of bacterial viability (**Figure 9**).

The results of this study offer a strong mechanistic basis for the continued development of Ag^+ as a novel antimicrobial agent. The systematic investigation of its antibacterial activity, combined with the identification of specific molecular targets, offers valuable insights for rational drug design. Notably, the low resistance frequency observed for Ag^+ compared to conventional antibiotics like amoxicillin positions it as a promising candidate for addressing the growing challenge of antimicrobial resistance. The multi-target nature of Ag^+ action, concurrently inhibiting several essential Mur enzymes, may contribute to its sustained efficacy and reduced susceptibility to resistance development. Additionally, our ABPP results further indicate that, beyond the Mur family, Ag^+ can target multiple proteins in *Staphylococcus aureus*. In future studies, we will further characterize these targets to fully elucidate antibacterial mechanism of Ag^+, which may represent a significant advantage over single-target antibiotics. Future exploration of additional molecular targets of Ag^+ may reveal complementary mechanisms of action, potentially identifying new antibacterial targets. Although both Ag^+ and amoxicillin exert antibacterial activity through the inhibition of bacterial cell wall synthesis, their combination exhibits a pronounced synergistic effect. This may be explained by the fact that Ag^+ directly impairs the activity of cytoplasmic

Open Access Article. Published on 23 April 2026. Downloaded on 6/26/2026 5:23:11 PM.
This article is licensed under a Creative Commons Attribution-NonCommercial 3.0 Unported Licence.

Chemical Science Accepted Manuscript

View Article Online
DOI: 10.1039/D6SC00255B

Mur family enzymes responsible for the initial stages of peptidoglycan precursor synthesis, whereas amoxicillin inhibits penicillin-binding proteins that mediate the later stages of cell wall assembly and cross-linking. This complementary targeting of two functionally connected yet spatially distinct components within the same essential pathway provides a plausible mechanistic basis for the observed synergy. Given its favorable resistance profile, the development of combination therapies incorporating Ag^+ alongside existing antibiotics warrants serious consideration. Such synergistic combinations could provide a powerful strategy for treating multidrug-resistant bacterial infections, potentially extending the clinical lifespan of current antibiotics (40). Furthermore, silver ions' ability to overcome common resistance strategies, such as biofilm formation, merits deeper investigation to fully exploit its therapeutic potential.

Conclusion

In conclusion, this study systematically elucidates the antibacterial mechanism of silver ions (Ag^+) against *Staphylococcus aureus*, including MRSA. Using chemoproteomic approaches, we identified MurB, MurC, and MurD as primary coordinate covalent targets of Ag^+, with specific cysteine residues serving as critical binding sites. We demonstrated that Ag^+ not only suppresses the expression of MurB and MurD but also directly inhibits the enzymatic activity of MurC, thereby disrupting peptidoglycan synthesis and compromising bacterial cell wall integrity. Electron microscopy confirmed extensive structural damage, including membrane thinning and cell wall rupture, following Ag^+ treatment. Notably, Ag^+ exhibits a remarkably low resistance frequency compared to conventional antibiotics and maintains potent efficacy against amoxicillin-resistant strains. Beyond its direct bactericidal effects, Ag^+ attenuates key virulence traits, including adhesion, invasion, and biofilm formation, while mitigating inflammatory responses in host cells. These results indicate that Ag^+ has a unique mechanism of action and could function as a valuable mechanistic probe, providing inspiration for Mur-targeted antibacterial design and offering important insights for developing new antibiotics to combat global bacterial resistance.

Open Access Article. Published on 23 April 2026. Downloaded on 6/26/2026 5:23:11 PM.
This article is licensed under a Creative Commons Attribution-NonCommercial 3.0 Unported Licence.

Chemical Science Accepted Manuscript

View Article Online
DOI: 10.1039/D6SC00255B

Open Access Article. Published on 23 April 2026. Downloaded on 6/26/2026 5:23:11 PM.
This article is licensed under a Creative Commons Attribution-NonCommercial 3.0 Unported Licence.

Author contributions

J. G. W., and H. T. designed and conceived the project. L. R. Z., and Y. Z. conducted the anti- *Staphylococcus aureus* experiments, collected the results, and written original draft. Y. J. L., and T. Y., carried out the molecular experiments. Z. C., and C. W., performed the bioinformatics analysis. Z. C., Q. Y. Z., and H. C. T., contributed to software and formal analysis. A. M., P. G., Y. K. W., C. L., S. N. S., J. Z. Z., and Q. L. S., contributes to the assessment of bacterial invasion. J. G. W., and H. T., revised the manuscript. All authors reviewed and approved the final version of the manuscript.

Conflicts of interest

The authors declare no conflicts of interest to disclose.

Data availability

All other data are included in the manuscript supporting information (SI). Supplementary information: instrumentation, methods, and supporting information figure.

Acknowledgment

This study was supported by the National Science and Technology Major Project of the Ministry of Science and Technology of China (2026ZD01910002), National Natural Science Foundation of China (82522095), the CACMS Innovation Fund (CI2025D002, CI2023E005TS01, and CI2024E003), China Central Government Guidance Funds for Local Science and Technology Development Projects (2025ZY0072), the China Fundamental Research Funds for the Central public welfare research institutes (ZZ14-YQ-061).

Reference

(1) Chen, X.; Schneewind, O.; Missiakas, D. Engineered human antibodies for the opsonization and

Chemical Science Accepted Manuscript

View Article Online
DOI: 10.1039/D6SC00255B

killing of Staphylococcus aureus. Proc Natl Acad Sci U S A 2022, 119 (4), DOI: 10.1073/pnas.2114478119.

(2) Howden, B. P.; Giulieri, S. G.; Wong Fok Lung, T.; Baines, S. L.; Sharkey, L. K.; Lee, J. Y. H.; Hachani, A.; Monk, I. R.; Stinear, T. P. Staphylococcus aureus host interactions and adaptation. Nat Rev Microbiol 2023, 21 (6), 380-395. DOI: 10.1038/s41579-023-00852-y.

(3) Lowy, F. D. Staphylococcus aureus infections. N Engl J Med 1998, 339 (8), 520-532. DOI: 10.1056/nejm199808203390806.

(4) Laxminarayan, R.; Matsoso, P.; Pant, S.; Brower, C.; Røttingen, J. A.; Klugman, K.; Davies, S. Access to effective antimicrobials: a worldwide challenge. Lancet 2016, 387 (10014), 168-175. DOI: 10.1016/s0140-6736(15)00474-2.

(5) Blaser, M. J. Antibiotic use and its consequences for the normal microbiome. Science 2016, 352 (6285), 544-545. DOI: 10.1126/science.aad9358.

(6) Palumbi, S. R. Humans as the world's greatest evolutionary force. Science 2001, 293 (5536), 1786-1790. DOI: 10.1126/science.293.5536.1786.

(7) Tong, S. Y.; Davis, J. S.; Eichenberger, E.; Holland, T. L.; Fowler, V. G., Jr. Staphylococcus aureus infections: epidemiology, pathophysiology, clinical manifestations, and management. Clin Microbiol Rev 2015, 28 (3), 603-661. DOI: 10.1128/cmr.00134-14.

(8) von Nussbaum, F.; Brands, M.; Hinzen, B.; Weigand, S.; Häbich, D. Antibacterial natural products in medicinal chemistry--exodus or revival? Angew Chem Int Ed Engl 2006, 45 (31), 5072-5129. DOI: 10.1002/anie.200600350.

(9) Krismer, B.; Weidenmaier, C.; Zipperer, A.; Peschel, A. The commensal lifestyle of Staphylococcus aureus and its interactions with the nasal microbiota. Nat Rev Microbiol 2017, 15 (11), 675-687. DOI: 10.1038/nrmicro.2017.104.

(10) Singh, N.; Rajwade, J.; Paknikar, K. M. Transcriptome analysis of silver nanoparticles treated Staphylococcus aureus reveals potential targets for biofilm inhibition. Colloids Surf B Biointerfaces 2019, 175, 487-497. DOI: 10.1016/j.colsurfb.2018.12.032.

(11) Liao, X.; Yang, F.; Wang, R.; He, X.; Li, H.; Kao, R. Y. T.; Xia, W.; Sun, H. Identification of catabolite control protein A from Staphylococcus aureus as a target of silver ions. Chem Sci 2017, 8 (12), 8061-8066. DOI: 10.1039/c7sc02251d.

(12) Lin, Y.; Liu, L.; He, J.; Shen, J.; Ren, Q. Rapid release of high-valent silver ions from water-soluble porphyrin complexes to enhance the direct killing of Methicillin-Resistant Staphylococcus aureus. Acta Biomater 2025, 192, 419-430. DOI: 10.1016/j.actbio.2024.12.004.

(13) Ueda, Y.; Miyazaki, M.; Mashima, K.; Takagi, S.; Hara, S.; Kamimura, H.; Jimi, S. The Effects of Silver Sulfadiazine on Methicillin-Resistant Staphylococcus aureus Biofilms. Microorganisms 2020, 8 (10). DOI: 10.3390/microorganisms8101551.

(14) Hao, H.; Cheng, G.; Dai, M.; Wu, Q.; Yuan, Z. Inhibitors targeting on cell wall biosynthesis pathway of MRSA. Mol Biosyst 2012, 8 (11), 2828-2838. DOI: 10.1039/c2mb25188d From NLM.

(15) Figueiredo, T. A.; Sobral, R. G.; Ludovice, A. M.; Almeida, J. M.; Bui, N. K.; Vollmer, W.; de Lencastre, H.; Tomasz, A. Identification of genetic determinants and enzymes involved with the amidation of glutamic acid residues in the peptidoglycan of Staphylococcus aureus. PLoS Pathog 2012, 8 (1), e1002508. DOI: 10.1371/journal.ppat.1002508.

(16) Kumari, M.; Subbarao, N. Identification of novel multitarget antitubercular inhibitors against mycobacterial peptidoglycan biosynthetic Mur enzymes by structure-based virtual screening. J Biomol Struct Dyn 2022, 40 (18), 8185-8196. DOI: 10.1080/07391102.2021.1908913.

Open Access Article. Published on 23 April 2026. Downloaded on 6/26/2026 5:23:11 PM.
This article is licensed under a Creative Commons Attribution-NonCommercial 3.0 Unported Licence.

Chemical Science Accepted Manuscript

View Article Online
DOI: 10.1039/D6SC00255B

(17) Laddomada, F.; Miyachiro, M. M.; Jessop, M.; Patin, D.; Job, V.; Mengin-Lecreulx, D.; Le Roy, A.; Ebel, C.; Breyton, C.; Gutsche, I.; et al. The MurG glycosyltransferase provides an oligomeric scaffold for the cytoplasmic steps of peptidoglycan biosynthesis in the human pathogen Bordetella pertussis. Sci Rep 2019, 9 (1), 4656. DOI: 10.1038/s41598-019-40966-z.

(18) Morlot, C.; Straume, D.; Peters, K.; Hegnar, O. A.; Simon, N.; Villard, A. M.; Contreras-Martel, C.; Leisico, F.; Breukink, E.; Gravier-Pelletier, C.; et al. Structure of the essential peptidoglycan amidotransferase MurT/GatD complex from Streptococcus pneumoniae. Nat Commun 2018, 9 (1), 3180. DOI: 10.1038/s41467-018-05602-w.

(19) Maitra, A.; Munshi, T.; Healy, J.; Martin, L. T.; Vollmer, W.; Keep, N. H.; Bhakta, S. Cell wall peptidoglycan in Mycobacterium tuberculosis: An Achilles' heel for the TB-causing pathogen. FEMS Microbiol Rev 2019, 43 (5), 548-575. DOI: 10.1093/femsre/fuz016.

(20) Liao, X.; Yang, F.; Li, H.; So, P. K.; Yao, Z.; Xia, W.; Sun, H. Targeting the Thioredoxin Reductase-Thioredoxin System from Staphylococcus aureus by Silver Ions. Inorg Chem 2017, 56 (24), 14823-14830. DOI: 10.1021/acs.inorgchem.7b01904.

(21) Koo, T. Y.; Lai, H.; Nomura, D. K.; Chung, C. Y. N-Acryloylindole-alkyne (NAIA) enables imaging and profiling new ligandable cysteines and oxidized thiols by chemoproteomics. Nat Commun 2023, 14 (1), 3564. DOI: 10.1038/s41467-023-39268-w.

(22) Yan, T.; Desai, H. S.; Boatner, L. M.; Yen, S. L.; Cao, J.; Palafox, M. F.; Jami-Alahmadi, Y.; Backus, K. M. SP3-FAIMS Chemoproteomics for High-Coverage Profiling of the Human Cysteinome*. Chembiochem 2021, 22 (10), 1841-1851. DOI: 10.1002/cbic.202000870.

(23) Wilkinson, I. V. L.; Bottlinger, M.; El Harraoui, Y.; Sieber, S. A. Profiling the Heme-Binding Proteomes of Bacteria Using Chemical Proteomics. Angew Chem Int Ed Engl 2023, 62 (9), e202212111. DOI: 10.1002/anie.202212111.

(24) Reinhardt, T.; Lee, K. M.; Niederegger, L.; Hess, C. R.; Sieber, S. A. Indolin-2-one Nitroimidazole Antibiotics Exhibit an Unexpected Dual Mode of Action. ACS Chem Biol 2022, 17 (11), 3077-3085. DOI: 10.1021/acschembio.2c00462.

(25) Rahman, M. A.; Amirkhani, A.; Parvin, F.; Chowdhury, D.; Molloy, M. P.; Deva, A. K.; Vickery, K.; Hu, H. One Step Forward with Dry Surface Biofilm (DSB) of Staphylococcus aureus: TMT-Based Quantitative Proteomic Analysis Reveals Proteomic Shifts between DSB and Hydrated Biofilm. Int J Mol Sci 2022, 23 (20). DOI: 10.3390/ijms232012238.

(26) Shinde, Y.; Ahmad, I.; Surana, S.; Patel, H. The Mur Enzymes Chink in the Armour of Mycobacterium tuberculosis cell wall. Eur J Med Chem 2021, 222, 113568. DOI: 10.1016/j.ejmech.2021.113568.

(27) Eniyan, K.; Kumar, A.; Rayasam, G. V.; Perdih, A.; Bajpai, U. Development of a one-pot assay for screening and identification of Mur pathway inhibitors in Mycobacterium tuberculosis. Sci Rep 2016, 6, 35134. DOI: 10.1038/srep35134.

(28) Liang, H.; DeMeester, K. E.; Hou, C. W.; Parent, M. A.; Caplan, J. L.; Grimes, C. L. Metabolic labelling of the carbohydrate core in bacterial peptidoglycan and its applications. Nat Commun 2017, 8, 15015. DOI: 10.1038/ncomms15015.

(29) Zhanel, G. G.; Golden, A. R.; Zelenitsky, S.; Wiebe, K.; Lawrence, C. K.; Adam, H. J.; Idowu, T.; Domalaon, R.; Schweizer, F.; Zhanel, M. A.; et al. Cefiderocol: A Siderophore Cephalosporin with Activity Against Carbapenem-Resistant and Multidrug-Resistant Gram-Negative Bacilli. Drugs 2019, 79 (3), 271-289. DOI: 10.1007/s40265-019-1055-2.

(30) Fan, Y.; Mohanty, S.; Zhang, Y.; Lüchow, M.; Qin, L.; Fortuin, L.; Brauner, A.; Malkoch, M.

Open Access Article. Published on 23 April 2026. Downloaded on 6/26/2026 5:23:11 PM.
This article is licensed under a Creative Commons Attribution-NonCommercial 3.0 Unported Licence.

Chemical Science Accepted Manuscript

View Article Online
DOI: 10.1039/D6SC00255B

Dendritic Hydrogels Induce Immune Modulation in Human Keratinocytes and Effectively Eradicate Bacterial Pathogens. J Am Chem Soc 2021, 143 (41), 17180-17190. DOI: 10.1021/jacs.1c07492.

(31) Blanco Massani, M.; To, D.; Meile, S.; Schmelcher, M.; Gintsburg, D.; Coraça-Huber, D. C.; Seybold, A.; Loessner, M.; Bernkop-Schnürch, A. Enzyme-responsive nanoparticles: enhancing the ability of endolysins to eradicate Staphylococcus aureus biofilm. J Mater Chem B 2024, 12 (37), 9199-9205. DOI: 10.1039/d4tb01122h.

(32) Yang, X.; Lan, W.; Xie, J. Antimicrobial and anti-biofilm activities of chlorogenic acid grafted chitosan against Staphylococcus aureus. Microb Pathog 2022, 173 (Pt A), 105748. DOI: 10.1016/j.micpath.2022.105748.

(33) Kouvela, A.; Jaramillo Ponce, J. R.; Giarimoglou, N.; Chicher, J.; Marzi, S.; Stathopoulos, C.; Stamatopoulou, V. Coupling tRNAGly gene redundancy with staphylococcal cell wall integrity, antibiotic susceptibility, and virulence potential. Nucleic Acids Res 2025, 53 (13). DOI: 10.1093/nar/gkaf599.

(34) Zhou, J.; Fu, R.; Tian, F.; Yang, Y.; Jiao, B.; He, Y. Dual Enzyme-Induced Au-Ag Alloy Nanorods as Colorful Chromogenic Substrates for Sensitive Detection of Staphylococcus aureus. ACS Appl Bio Mater 2020, 3 (9), 6103-6109. DOI: 10.1021/acsabm.0c00687.

(35) Chen, J.; Zhou, H.; Huang, J.; Zhang, R.; Rao, X. Virulence alterations in staphylococcus aureus upon treatment with the sub-inhibitory concentrations of antibiotics. J Adv Res 2021, 31, 165-175. DOI: 10.1016/j.jare.2021.01.008.

(36) Yoshii, Y.; Okuda, K. I.; Yamada, S.; Nagakura, M.; Sugimoto, S.; Nagano, T.; Okabe, T.; Kojima, H.; Iwamoto, T.; Kuwano, K.; et al. Norgestimate inhibits staphylococcal biofilm formation and resensitizes methicillin-resistant Staphylococcus aureus to β-lactam antibiotics. NPJ Biofilms Microbiomes 2017, 3, 18. DOI: 10.1038/s41522-017-0026-1.

(37) Butucel, E.; Balta, I.; Bundurus, I. A.; Popescu, C. A.; Iancu, T.; Venig, A.; Pet, I.; Stef, D.; McCleery, D.; Stef, L.; et al. Natural Antimicrobials Promote the Anti-Oxidative Inhibition of COX-2 Mediated Inflammatory Response in Primary Oral Cells Infected with Staphylococcus aureus, Streptococcus pyogenes and Enterococcus faecalis. Antioxidants (Basel) 2023, 12 (5). DOI: 10.3390/antiox12051017.

(38) Merghni, A.; Hamdi, H.; Ben Abdallah, M.; Al-Hasawi, Z. M.; Al-Quwaie, D. A.; Abid-Essefi, S. Detection of Methicillin-Resistant Staphylococcus aureus among Foodborne Pathogenic Strains and Assessment of Their Adhesion Ability and Cytotoxic Effects in HCT-116 Cells. Foods 2023, 12 (5). DOI: 10.3390/foods12050974.

(39) Ignatova, N.; Abidullina, A.; Streltsova, O.; Elagin, V.; Kamensky, V. Norepinephrine Effects on Uropathogenic Strains Virulence. Microorganisms 2022, 10 (11). DOI: 10.3390/microorganisms10112248.

(40) Liu, W.; Zhang, H.; Dong, X.; Sun, Y. Composite of gold nanoclusters and basified human serum albumin significantly boosts the inhibition of Alzheimer's β-amyloid by photo-oxygenation. Acta Biomater 2022, 144, 157-167. DOI: 10.1016/j.actbio.2022.03.019.

(41) Brdová, D.; Ruml, T.; Viktorová, J. Mechanism of staphylococcal resistance to clinically relevant antibiotics. Drug Resist Updat 2024, 77, 101147. DOI: 10.1016/j.drup.2024.101147.

(42) Nathan, C.; Cars, O. Antibiotic resistance--problems, progress, and prospects. N Engl J Med 2014, 371 (19), 1761-1763. DOI: 10.1056/NEJMp1408040.

(43) Lázár, V.; Snitser, O.; Barkan, D.; Kishony, R. Antibiotic combinations reduce Staphylococcus aureus clearance. Nature 2022, 610 (7932), 540-546. DOI: 10.1038/s41586-022-05260-5.

Open Access Article. Published on 23 April 2026. Downloaded on 6/26/2026 5:23:11 PM.
This article is licensed under a Creative Commons Attribution-NonCommercial 3.0 Unported Licence.

Chemical Science Accepted Manuscript

(44) Kumar, G.; Engle, K. Natural products acting against S. aureus through membrane and cell wall disruption. Nat Prod Rep 2023, 40 (10), 1608-1646. DOI: 10.1039/d2np00084a.

View Article Online
DOI: 10.1039/D6SC00255B

Open Access Article. Published on 23 April 2026. Downloaded on 6/26/2026 5:23:11 PM.
This article is licensed under a Creative Commons Attribution-NonCommercial 3.0 Unported Licence.

Chemical Science Accepted Manuscript

View Article Online
DOI: 10.1039/D6SC00255B

Open Access Article. Published on 23 April 2026. Downloaded on 6/26/2026 5:23:11 PM.
This article is licensed under a Creative Commons Attribution-NonCommercial 3.0 Unported Licence.

Chemical Science Accepted Manuscript

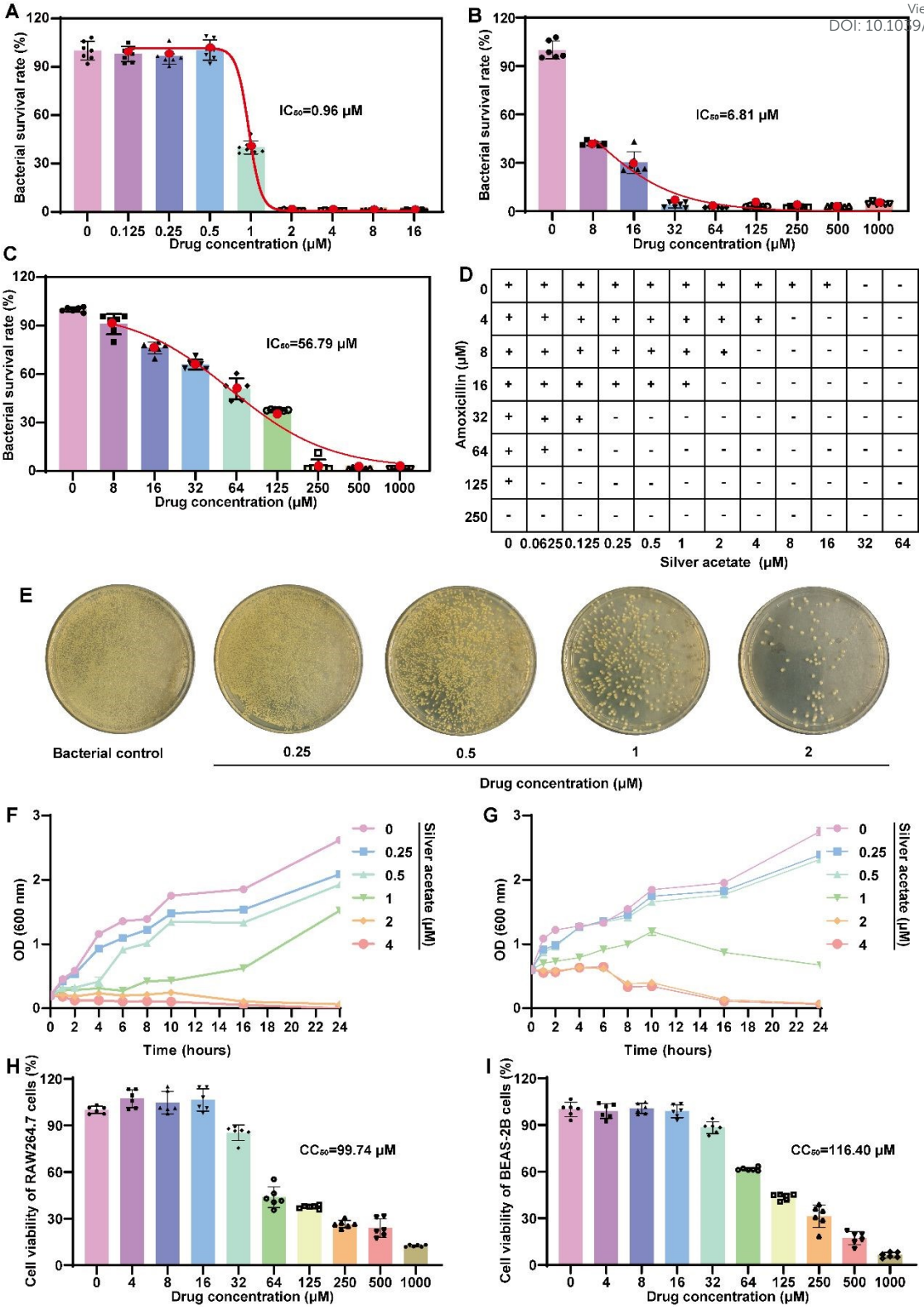

Figure 1. Ag^+ selectively killed bacteria with limited cytotoxicity on human cells. (A) Bacterial survival rate of *S. aureus* following 24 h of treatment with Ag^+ at various concentrations (n = 6). (B) Bacterial survival rate of methicillin-resistant *S. aureus* (MRSA) following 24 h of treatment with Ag^+ at various concentrations (n = 6). (C) Bacterial survival rate of Methicillin-resistant *S. aureus* (MRSA) following 24 h of treatment with amoxicillin at different concentrations (n = 6). (D) The checkerboard method showing the synergy of Ag^+ and amoxicillin combination. FIC =

View Article Online
DOI: 10.1039/D6SC00255B

(MIC of Ag^+ in combination / MIC of Ag^+ alone) + (MIC of Amoxicillin in combination / MIC of Amoxicillin alone) (E) Optical images of *S. aureus* colonies after 6 h of treatment with Ag^+ at different concentrations. (F) Growth curve of *S. aureus* over 24 h of treatment with Ag^+ at different concentrations (n = 3). (G) Killing curve of *S. aureus* over 24 h of treatment with Ag^+ at various concentrations (n = 3). (H) Cell viability of RAW cells following 24 h of treatment with Ag^+ at different concentrations (n = 6). (I) Cell viability of BEAS-2B cells following 24 h of treatment with Ag^+ at different concentrations (n = 6).

Open Access Article. Published on 23 April 2026. Downloaded on 6/26/2026 5:23:11 PM.
This article is licensed under a Creative Commons Attribution-NonCommercial 3.0 Unported Licence.

Chemical Science Accepted Manuscript

View Article Online
DOI: 10.1039/D6SC00255B

Open Access Article. Published on 23 April 2026. Downloaded on 6/26/2026 5:23:11 PM.
This article is licensed under a Creative Commons Attribution-NonCommercial 3.0 Unported Licence.

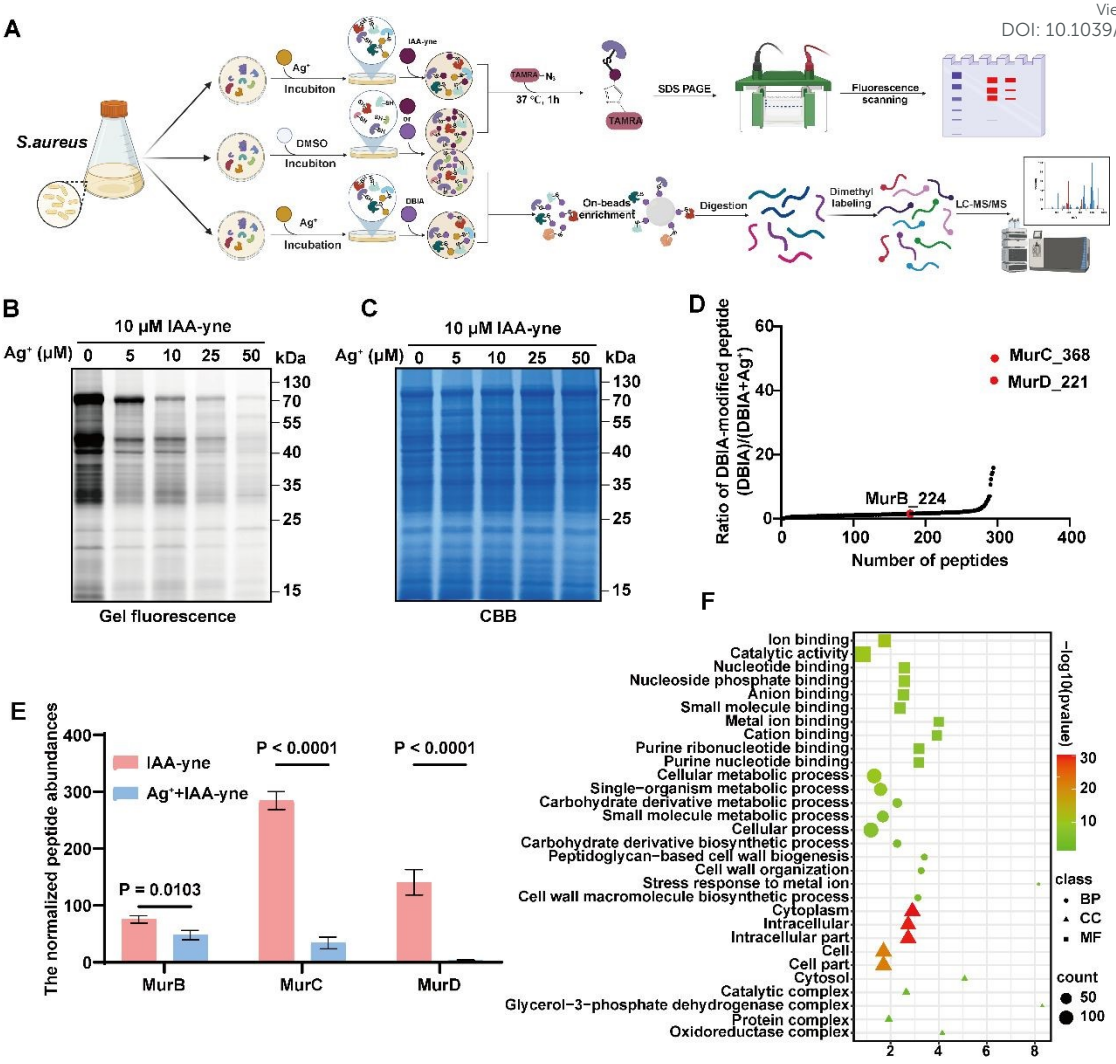

Figure 2. Protein target identification of Ag^+ in *S. aureus* via quantitative chemoproteomic profiling. (A) Overview of the workflow for profiling protein targets of Ag^+ in *S. aureus*. (B) Competitive fluorescent labeling of proteins in *S. aureus* by IAA-yne following *in situ* treatment in the presence of excess Ag^+. (C) Coomassie Brilliant Blue (CBB) staining was used to normalize the total protein content in panel (B). (D) Identification of potential Ag^+ targets in *S. aureus* through activity-based protein profiling. (The quantified signal represents relative cysteine reactivity, calculated as the normalized peptide intensity ratio between DBIA and DBIA+Ag^+-treated samples) (E) The normalized abundances of MurB, MurC, and MurD peptides targeted by Ag+. Proteome Discoverer software was used to standardize the intensity values were normalized across samples based on total peptide signal to enable comparison between different conditions (n = 3). (F) Gene Ontology (GO) pathway enrichment analysis of Ag^+-targeted proteins.

Chemical Science Accepted Manuscript

View Article Online
DOI: 10.1039/D6SC00255B

Open Access Article. Published on 23 April 2026. Downloaded on 6/26/2026 5:23:11 PM.
This article is licensed under a Creative Commons Attribution-NonCommercial 3.0 Unported Licence.

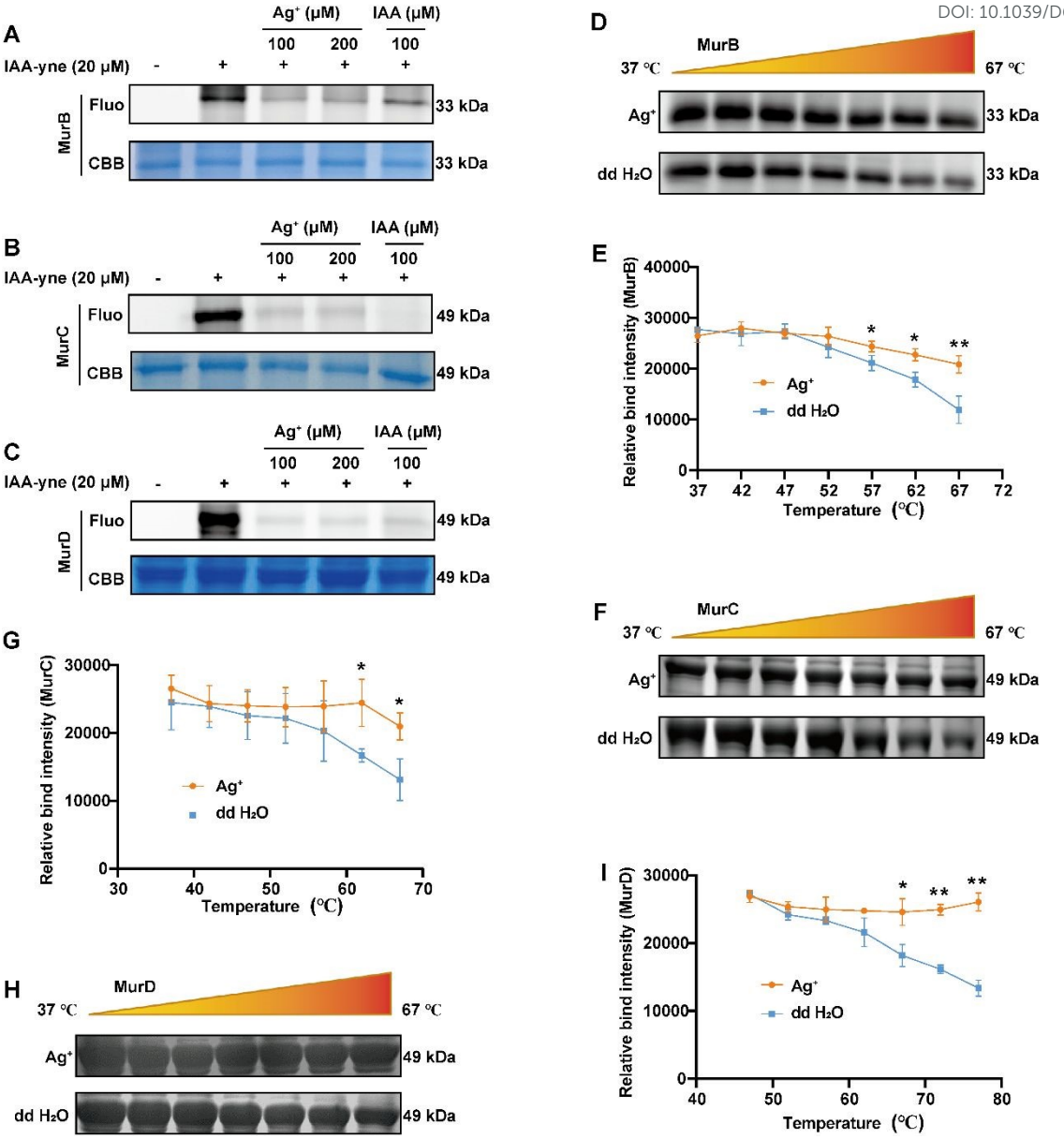

Figure 3. Protein target (murB, murC, murD) verification of Ag^+ in *S. aureus*. (A-C) Ag^+ competed away with IAA-yne probe for binding to purified recombinant MurB(A), MurC(B) and MurD(C) protein in a gel fluorescence assay. (D-E) Protein-based thermal shift assays showing the thermal stability of MurB in the absence and presence of Ag^+ (1 μM) (n = 3). (F-G) Protein-based thermal shift assays showing the thermal stability of MurC in the absence and presence of Ag^+ (1 μM) (n = 3). (H-I) Protein-based thermal shift assays showing the thermal stability of MurD in the absence and presence of Ag^+ (1 μM) (n = 3). Values are expressed as the mean ± SEM.

Chemical Science Accepted Manuscript

View Article Online
DOI: 10.1039/D6SC00255B

Open Access Article. Published on 23 April 2026. Downloaded on 6/26/2026 5:23:11 PM.
This article is licensed under a Creative Commons Attribution-NonCommercial 3.0 Unported Licence.

Chemical Science Accepted Manuscript

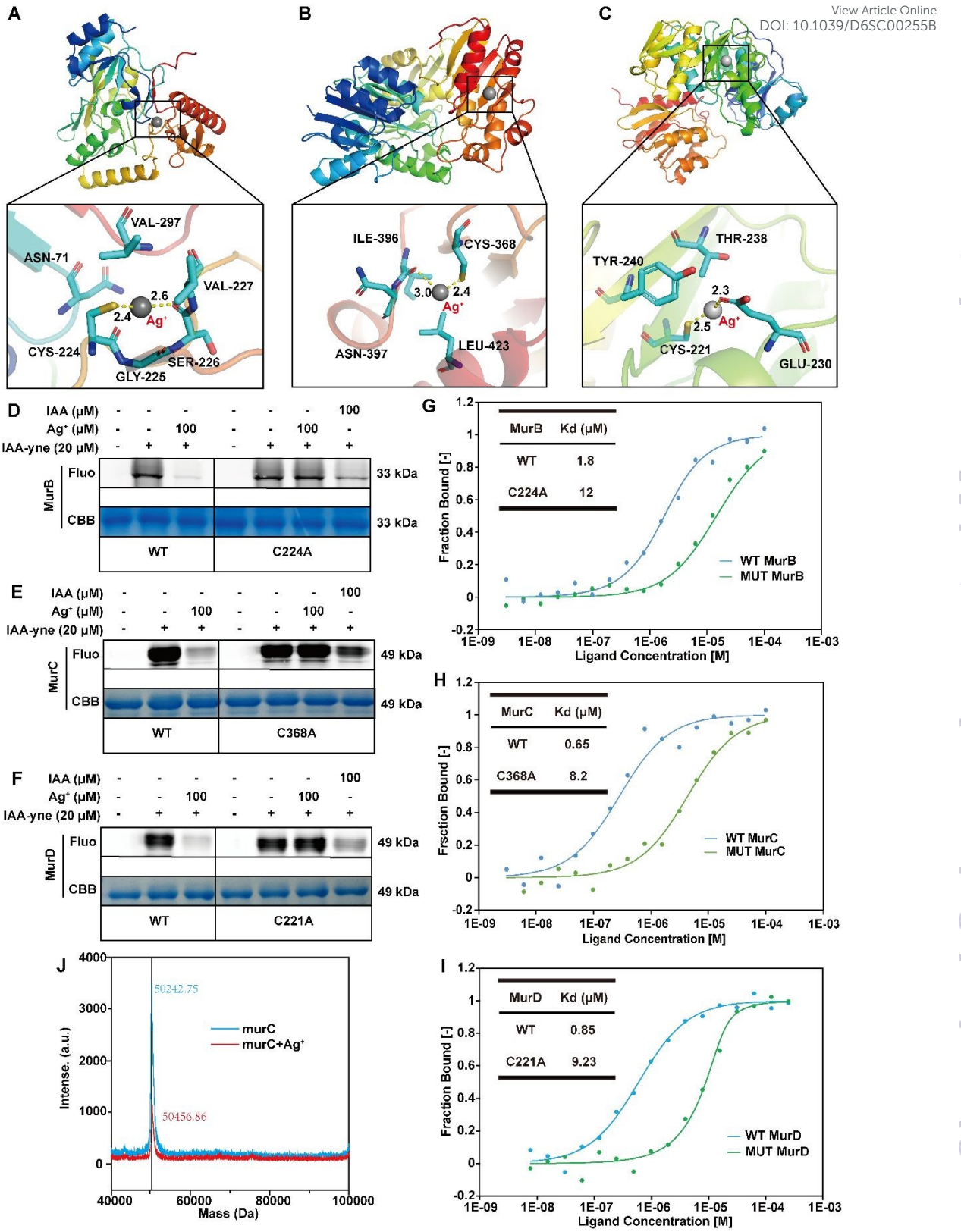

Figure 4. Ag^+ bind MurB, MurC and MurD at Cys224, Cys368 and Cys221. (A-C) A model of Ag^+ binding to the MurB(A), MurC(B) and MurD(C) protein, generated by molecular docking. (D) Ag^+ competed away with IAA-yne for binding to purified recombinant wild-type (WT) MurB and mutant MurB (C224A) protein in a gel fluorescence assay. (E) Ag^+ competed away with the IAA probe for binding to purified recombinant WT MurC and mutant MurC (C368A) protein in a gel

View Article Online
DOI: 10.1039/D6SC00255B

fluorescence assay. (F) Ag^+ competed away with IAA-yne for binding to purified recombinant WT MurD and mutant MurD (C221A) protein in a gel fluorescence assay. (G) The coordinate-covalent-type binding affinity of WT MurB and its mutant MurB (C224A) to Ag^+, measured by microscale thermophoresis. (H) The coordinate-covalent-type binding affinity of WT MurC and its mutant MurC (C368A) to Ag^+, measured by microscale thermophoresis. (I) The coordinate-covalent-type binding affinity of WT MurD and its mutant MurD (C221A) to Ag^+, measured by microscale thermophoresis. (J) Native mass spectra of murC in the absence (blue) and presence of Ag^+ (red) detected by MALDI-TOF.

Open Access Article. Published on 23 April 2026. Downloaded on 6/26/2026 5:23:11 PM.
This article is licensed under a Creative Commons Attribution-NonCommercial 3.0 Unported Licence.

Chemical Science Accepted Manuscript

View Article Online
DOI: 10.1039/D6SC00255B

Open Access Article. Published on 23 April 2026. Downloaded on 6/26/2026 5:23:11 PM.
This article is licensed under a Creative Commons Attribution-NonCommercial 3.0 Unported Licence.

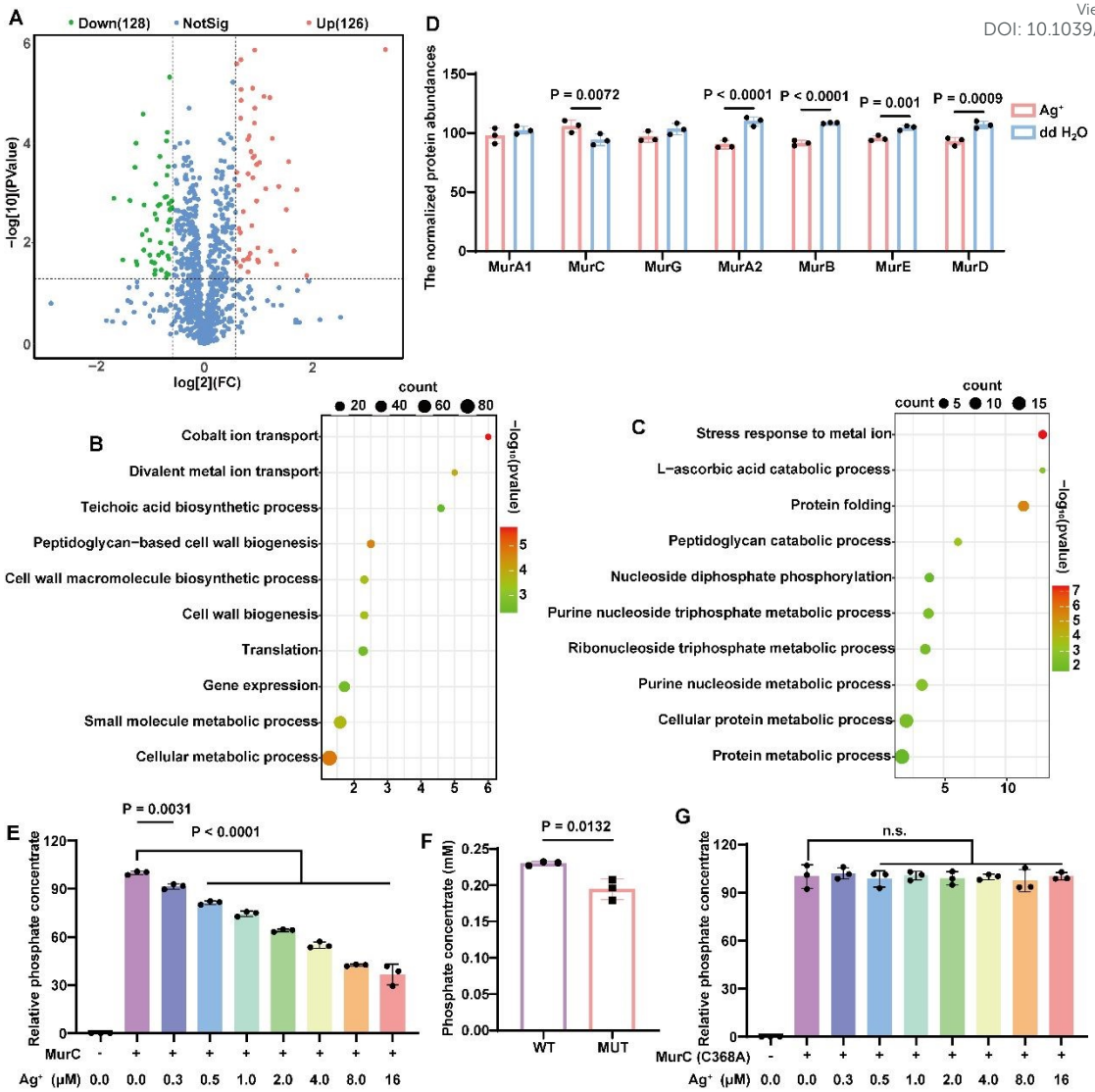

Figure 5. Ag^+ reduces the expression of MurB and MurD, as well as the enzymatic activity of MurC, by binding to MurB, MurC, and MurD proteins. (A) Volcano plot showing up-regulated genes (red dots) and down-regulated genes (green dots) in *S. aureus* treated with Ag^+, as determined by proteomics. (B) Gene Ontology (GO) analysis of up-regulated proteins in Ag^+-treated *S. aureus*. (C) GO analysis of down-regulated proteins in Ag^+-treated *S. aureus*. (D) Comparison of mur family protein expression levels in *S. aureus* in the presence and absence of Ag^+. Proteome Discoverer software was used to standardize the intensity values were normalized across samples based on total protein signal to enable comparison between different conditions (n = 3). (E) Effects of different concentrations of Ag^+ on the enzymatic activity of wild-type (WT) MurC protein (n = 3). (F) Comparison of enzyme activity before and after mutation at the CYS368 site of MurC (n = 3). (G) Effects of different concentrations of Ag^+ on the enzymatic activity of mutant (MUT) MurC (C368A) protein (n = 3). Values are expressed as the mean ± SEM.

Chemical Science Accepted Manuscript

View Article Online
DOI: 10.1039/D6SC00255B

Open Access Article. Published on 23 April 2026. Downloaded on 6/26/2026 5:23:11 PM.
This article is licensed under a Creative Commons Attribution-NonCommercial 3.0 Unported Licence.

Chemical Science Accepted Manuscript

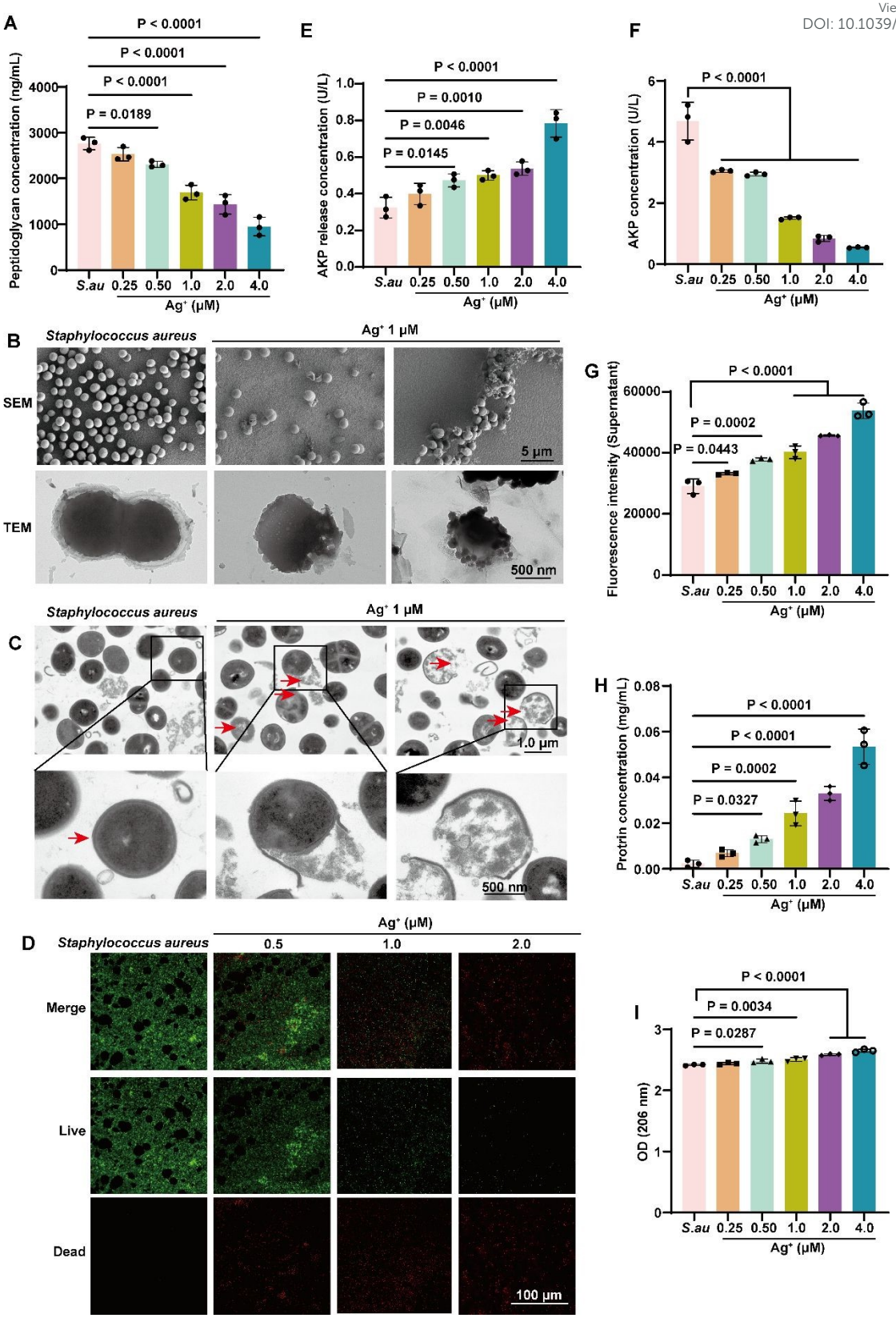

Figure 6. Ag^+ significantly inhibited the synthesis of peptidoglycan, disrupting the bacterial wall. (A) Peptidoglycan concentration in *S. aureus* following 10 h of treatment with Ag^+ at various concentrations (n = 3). (B) Morphological characterization of *S. aureus* following 10 h of treatment with Ag^+ at different concentrations, as observed by scanning electron microscopy (SEM) and

View Article Online
DOI: 10.1039/D6SC00255B

transmission electron microscopy (TEM). (C) Bacterial wall characterization of *S. aureus* following 10 h of treatment with Ag^+ at different concentrations observed by TEM. (D) Fluorescence imaging showing the live and dead status of *S. aureus* following 10 h of treatment with Ag^+ at different concentrations. Live and dead cells are indicated by green and red fluorescence, respectively. (E) Alkaline phosphatase (AKP) concentration in *S. aureus* culture medium following 6 h of treatment with Ag^+ at different concentrations (n = 3). (F) AKP concentration in *S. aureus* following 6 h of treatment with Ag^+ at different concentrations (n = 3). (G) Fluorescence intensity of *S. aureus* supernatant following 6 h of treatment with Ag^+ at different concentrations (n = 3). (H) Protein concentration in *S. aureus* culture medium following 6 h of treatment with Ag^+ at different concentrations (n = 3). (I) Nucleic acid concentration in *S. aureus* culture medium following 6 h of treatment with Ag^+ at different concentrations (n = 3). Values are expressed as the mean ± SEM.

Open Access Article. Published on 23 April 2026. Downloaded on 6/26/2026 5:23:11 PM.
This article is licensed under a Creative Commons Attribution-NonCommercial 3.0 Unported Licence.

Chemical Science Accepted Manuscript

View Article Online
DOI: 10.1039/D6SC00255B

Open Access Article. Published on 23 April 2026. Downloaded on 6/26/2026 5:23:11 PM.
This article is licensed under a Creative Commons Attribution-NonCommercial 3.0 Unported Licence.

Chemical Science Accepted Manuscript

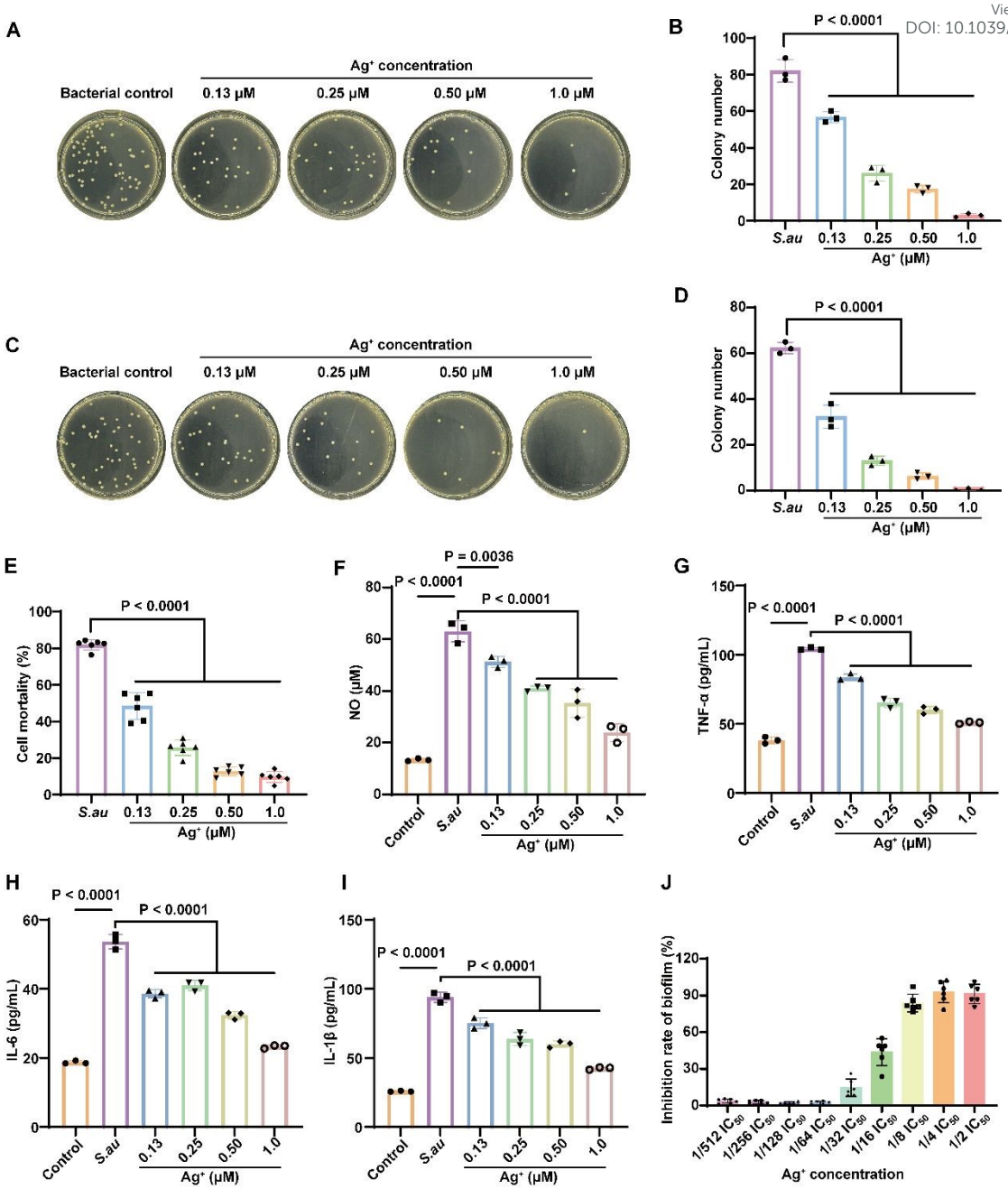

Figure 7. Ag^+ significantly reduced the pathogenicity of *S. aureus*. (A) After 4 h of treatment with Ag^+, optical images of *S. aureus* colonies adhering to BEAS-2B cells for 3 h was measured at various concentrations (n = 3). (B) After 4 hours of treatment with Ag^+, colony count of *S. aureus* adhering to BEAS-2B cells for 3 h was measured at various concentrations (n = 3). (C) After 4 h of treatment with Ag^+, optical images of *S. aureus* colonies invading to BEAS-2B cells for 3 h was measured at various concentrations (n = 3). (D) After 4 h of treatment with Ag^+, colony count of *S. aureus* invading to BEAS-2B cells for 3 hours was measured at various concentrations (n = 3). (E) BEAS-2B cells mortality following 24 h infection with *S. aureus* pretreated with different concentrations of Ag^+ for 4 h. (n = 6). (F-I) NO (F), TNF-α (G), IL-6 (H), and IL-1β (I) levels in the cell supernatant following 24 h infection with *S. aureus* pretreated with different concentrations of Ag^+ for 4 h. (n = 3). (J) Biofilm formation by *S. aureus* following 48 h of treatment with Ag^+ at different concentrations (n = 6). Values are expressed as the mean ± SEM.

View Article Online
DOI: 10.1039/D6SC00255B

Open Access Article. Published on 23 April 2026. Downloaded on 6/26/2026 5:23:11 PM.
This article is licensed under a Creative Commons Attribution-NonCommercial 3.0 Unported Licence.

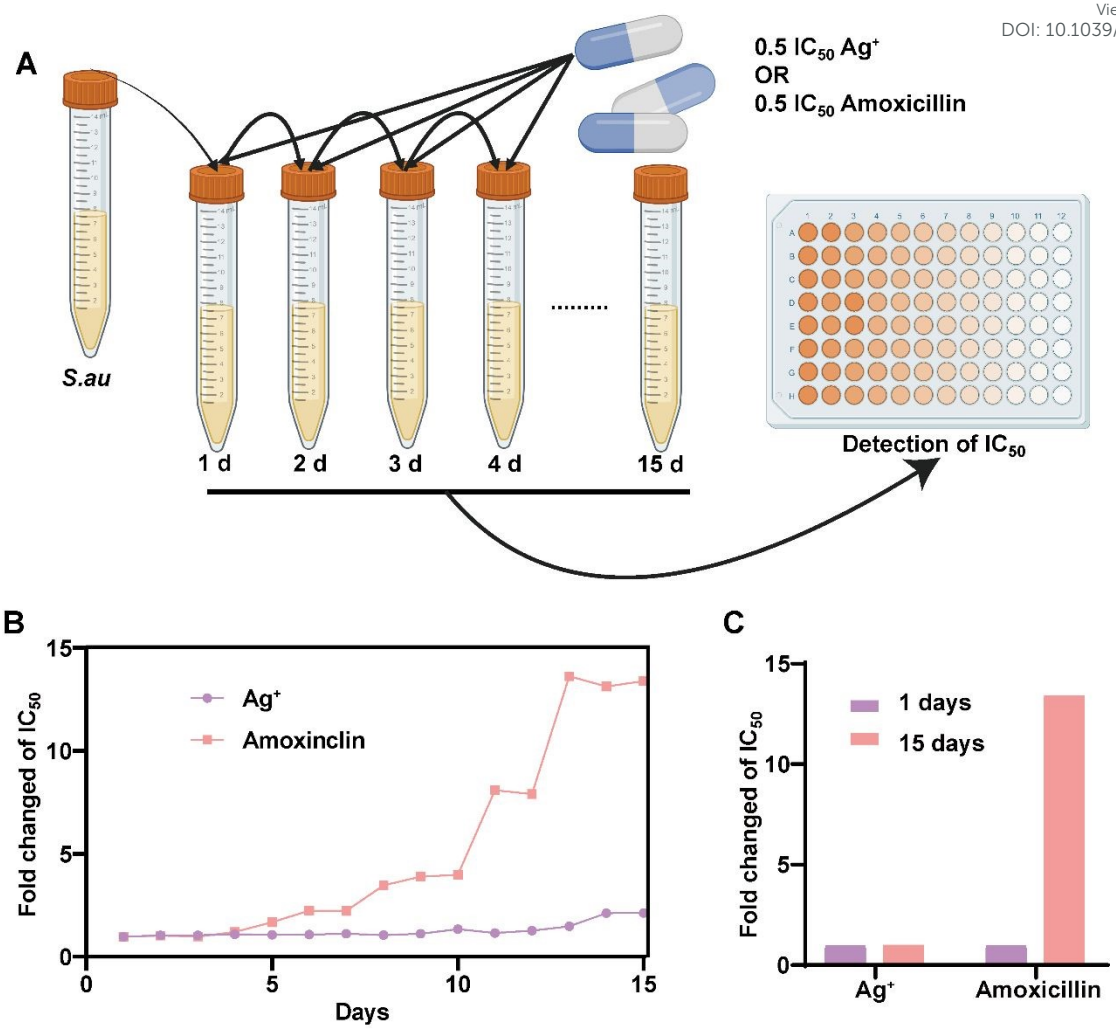

Figure 8. Low resistance development of Ag^+ for *S. aureus* treatment. (A-B) Exposure of *S. aureus* to IC_{50} dosing of Ag^+ and amoxicillin for 14 sequential passages (A) and the corresponding IC_{50} values (B). (C) The sensitivity of *S. aureus* to Ag^+ after 14 sequential cycles of treatment with IC_{50} dosing of amoxicillin.

Chemical Science Accepted Manuscript

View Article Online
DOI: 10.1039/D6SC00255B

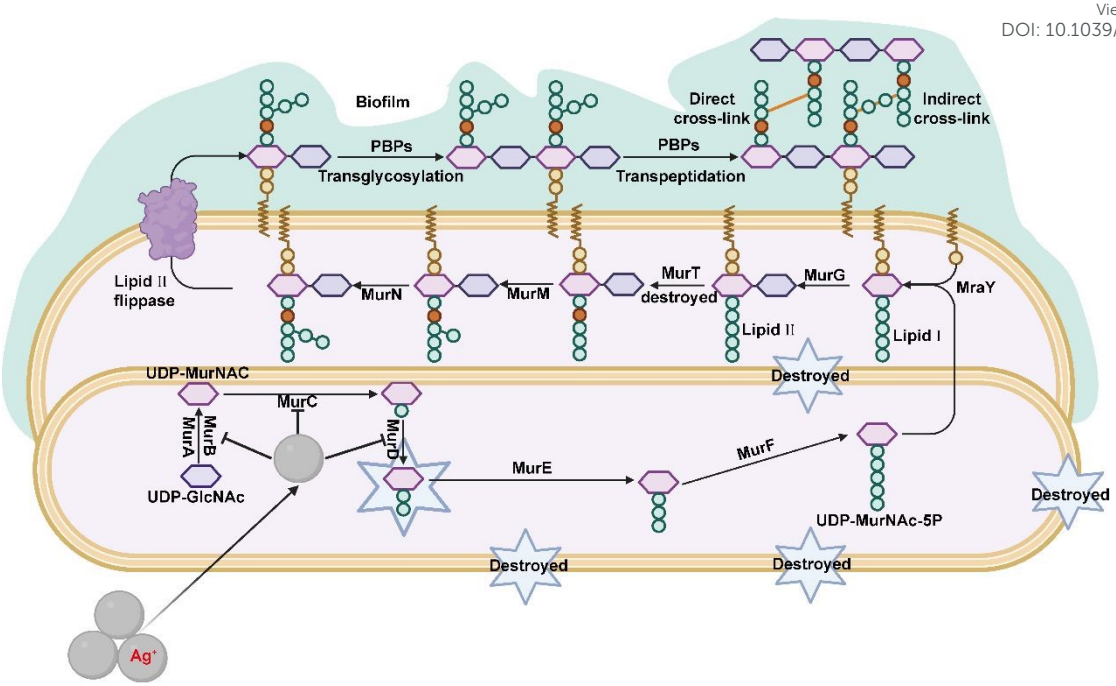

Figure 9. Schematic Diagram of Ag^+ Inhibition of *S. aureus*. This figure illustrates the mechanism by which Ag^+ inhibits *S. aureus* growth and pathogenicity. Ag^+ binds to key targets in *S. aureus*, including MurB, MurC, and MurD proteins, disrupting peptidoglycan synthesis and cell wall formation. This inhibition weakens the bacterial structure, reducing biofilm formation, impairing bacterial adhesion and invasion, and ultimately decreasing the pathogenicity of *S. aureus*.

Open Access Article. Published on 23 April 2026. Downloaded on 6/26/2026 5:23:11 PM.
This article is licensed under a Creative Commons Attribution-NonCommercial 3.0 Unported Licence.

Chemical Science Accepted Manuscript

View Article Online
DOI: 10.1039/D6SC00255B

The data that support the findings of this study are available from the corresponding author upon reasonable request.

Open Access Article. Published on 23 April 2026. Downloaded on 6/26/2026 5:23:11 PM.
This article is licensed under a Creative Commons Attribution-NonCommercial 3.0 Unported Licence.

Chemical Science Accepted Manuscript